Clinicopathological Manifestations and Immune Phenotypes in Adult-onset Immunodeficiency With Anti-interferon-γ Autoantibodies

Yi-Chun Chen
Division of Infectious Diseases, Department of Internal Medicine, Kaohsiung Chang Gung Memorial Hospital, Kaohsiung 83301, Taiwan

Shao-Wen Weng
Department of Internal Medicine, Kaohsiung Chang Gung Memorial Hospital, Kaohsiung 83301, Taiwan

Chen-Hsiang Lee
Division of Infectious Diseases, Department of Internal Medicine, Kaohsiung Chang Gung Memorial Hospital, Kaohsiung 83301, Taiwan

Wen-Chi Huang
Division of Infectious Diseases, Department of Internal Medicine, Kaohsiung Chang Gung Memorial Hospital, Kaohsiung 83301, Taiwan

Huey-Ling You
Department of Laboratory Medicine, Kaohsiung Chang Gung Memorial Hospital and Chang Gung University College of Medicine, Kaohsiung 83301, Taiwan

Wan-Ting Huang (huangwanting5@gmail.com)
Department of Laboratory Medicine, Kaohsiung Chang Gung Memorial Hospital and Chang Gung University College of Medicine, Kaohsiung 83301, Taiwan https://orcid.org/0000-0001-6442-3713

Research Article

Keywords: adult-onset immunodeficiency, anti-interferon-γ autoantibody, lymphocyte subpopulations, cytokine production

Posted Date: June 4th, 2021

DOI: https://doi.org/10.21203/rs.3.rs-562260/v1

Abstract

Purpose Adult-onset immunodeficiency with anti-interferon (IFN)-γ autoantibodies (anti-IFN-γ Abs) is an immunodeficiency syndrome. Immune dysfunction in this distinct disorder remains to be clarified.

Methods We prospectively collected blood samples of 20 patients with anti-IFN-γ Abs and 65 healthy normal subjects. Percentages of lymphocyte subpopulations, most relevant to T-, B-, and NK-cells, and percentages of stimulated lymphocytes with cytokine production were assessed using eight-color flow cytometry. The results were adjusted to age and absolute lymphocyte counts.

Results Most (85%) patients presented non-tuberculous mycobacterial infection. Skin lesions were predominantly manifested by neutrophilic dermatoses. Involved lymph nodes had granulomatous inflammation, except 22.2% showing atypical lymphoid hyperplasia without granuloma formation. In the multiple linear regression model, CD4+ T cells and non-activated subpopulations (recent thymic emigrants and naïve subtypes) were significantly decreased with increased expression of activation markers and polarization to Th1, Th17, and Treg. The percentage of NK cells was increased, but two major NK subpopulations, $CD56^{bright}$ and CD56+CD16+ subsets were decreased. Furthermore, NK cells diminished expression of NKp30 and NKp46 with increased CD57 expression. The cytokine production was significantly lower, namely TNF-α in CD4+ T cells ($P = 0.009$), CD8+ T cells ($P < 0.001$), and NK cells ($P = 0.002$); IFN-γ in CD8+ T cells ($P = 0.002$) and NK cells ($P = 0.001$); and IL-2 in CD4+ ($P < 0.001$), and CD8+ ($P = 0.005$) T cells.

Conclusion We conclude that the immune system in patients with anti–IFN-γ Abs could be exhausted which may contribute to the distinct clinicopathologic features.

Introduction

Adult-onset immunodeficiency due to anti-interferon (IFN)-γ autoantibodies (anti-IFN-γ Abs) is a distinct disorder, recently emerging in Asia [1, 2]. Thus far more than 500 patients with anti-IFN-γ Abs have been described [3]. Almost all patients are adults aged 30 to 70 years with no sex predominance [1, 3]. Neutralizing anti-IFN-γ Abs are responsible for the increased susceptibility to infections of nontuberculous mycobacteria (NTM) and intracellular pathogens. Of the body systems, lymph nodes were most commonly involved followed by skin [4]. Besides direct infections, reactive conditions such as skin manifestation were frequent, with reactive skin disorders, mostly neutrophilic dermatoses, were reported in 82% of the patients [5]. Early diagnosis of the disease is difficult due to protean manifestations in immunocompetent hosts and the absence of reproducible laboratory assays [6]. Patients may require long-term antimycobacterial therapy due to chronic infections and high recurrence rates, even after remission [7].

IFN-γ is produced by CD4 + T cells, CD8 + T cells, and natural killer (NK) cells, which target monocytes, macrophages, and neutrophils, in addition to nonprofessional host defense cells such as fibroblasts, hepatocytes, astrocytes, microglia, and endothelial cells [8]. It plays a critical regulatory role in macrophage-mediated killing and granuloma formation in response to intracellular pathogens. Over the past one and a half decades, anti-IFN-γ Abs have been reported to be associated with disseminated NTM and other opportunistic infections, including *Salmonella* species, *Talaromyces marneffei* and varicella-zoster virus [2]. Titers of anti-IFN-γ Abs may reflect disease activity [7], however, the pathogenesis of anti-IFN-γ Abs associated with immunodeficiency syndrome remains elusive. A previous study reported that the presence of anti-IFN-γ Abs had immunosuppressive effects in both innate and adaptive immunity. This is done by blocking IFN-γ activated STAT1 activation, IRF1 transactivation, and the production of chemokine and cytokine [9], putting a stop to IFN-γ-induced immunomodulation and antimicrobial activities.

Some studies highlighted alterations of lymphocyte subpopulations in patients with anti-IFN-γ Abs. The percentages of T cells and naïve subsets were decreased, while the number of NK cells was increased [1, 10]. Decreased abilities of lymphocyte subpopulations to produce TNF-α, IFN-γ, and IL-2 were reported [9, 11], however, a comprehensive analysis of lymphocyte subpopulations and activities was limited. In this study, we have not only described the clinicopathologic features of 20 patients with anti-IFN-γ Abs but analyzed most relevant T-, B-, and NK-cell subpopulations using eight-color flow cytometry. Percentages of stimulated lymphocyte subsets producing cytokines were evaluated. Our results suggest that the immune dysfunction of adult-onset immunodeficiency due to anti-IFN-γ Abs may be associated with decreased thymic output and immune exhaustion.

Material And Methods

Study population

Twenty patients with anti-IFN-γ Abs were diagnosed at Chang Gung Memorial Hospital in Kaohsiung, Taiwan. The determination of anti-IFN-γ Abs in plasma was carried out using methods as previously reported [12, 13]. All patients were HIV negative. Sixty-five healthy normal subjects with no evidence of immunosuppression were included as a control group. Demographic and clinical data of all enrolled patients were collected. The hematoxylin and eosin-stained sections obtained at the time of diagnosis and repeats were reviewed by the pathologist. This study was approved by the Ethics Committee of Chang Gung Memorial Hospital, Kaohsiung, Taiwan, in accordance with the Declaration of Helsinki (IRB201901509B0C501). Written informed consent was obtained from all subjects prior to enrollment.

Lymphocyte subpopulations by flow cytometric analysis

EDTA-anticoagulated whole blood samples were collected for the flow cytometry study. A staining volume of 100 µl peripheral blood mononuclear cells (PBMCs) separated by centrifugation was incubated with an antibody cocktail (BD Biosciences, Heidelberg, Germany) (Table 1). The eight-color staining panels for lymphocyte subpopulations were set and analyzed as previously reported [14]. The panels discriminated subsets from lymphocyte populations to assess (1) the general lymphocyte overview; (2) B-cell subpopulations; (3) CD4 + T-cell subpopulations; (4) CD8 + T-cell subpopulations; (5) regulatory T cells; (6) recent thymic emigrants (RTEs); (7) NK-cell subpopulations; and (8) NK-cell activation markers. After incubation for 20 min at room temperature (23°C) in the dark, red blood cells (RBCs) were lysed using lysis buffer (BD Biosciences) for 10 min. Following centrifugation and washing with fetal bovine serum (PBS), cells were fixed with 200 µl PBS containing 1% formaldehyde and stored at 4°C in a dark chamber until flow cytometry analysis. We used a FACS Canto II flow cytometer (BD Biosciences) equipped with three lasers (405 nm violet laser, 488 nm blue laser, and 647 nm red laser) for data acquisition and FACS DIVA software (BD Biosciences) for data analysis.

Table 1
Description of antibodies used for the flow cytometry study

Antibody	Panels	Clone	Vendor	Fluorophores	Antibody (uL)/100uL blood
CD45	All panels, cytokine	2D1	BD Pharmingen	APC-H7	2.5, 5*
CD3	I, III, IV, V VI, VII, VIII	UCHT1	BD Horizon	V500	2.5
CD3	Cytokine	SK7	BD Biosciences	FITC	20*
CD4	I, VI, cytokine	L200	BD Horizon	V450, BV421	2.5, 5*
CD4	III, V	SK3	BD Horizon	V450	2.5
CD8	I, cytokine	SK1	BD Pharmingen	PerCP-Cy5.5, APC	5, 5*
CD8	IV	RPA-T8	BD Horizon	V450	2.5
CD19	I	SJ25C1	BD Biosciences	APC	2.5
CD19	II	HIB19	BD Horizon	V500	2.5
CD16	I, VIII, cytokine	B73.1	BD Biosciences	PE-Cy7	2.5, 5*
CD16	VII	3G8	BD Horizon	V450	2.5
CD56	I, VIII, cytokine	NCAM16.2	BD Biosciences	PE-Cy7	2.5, 5*
CD38	I, II	HB7	BD Biosciences	PE, PE-Cy7	5, 2.5
HLA-DR	I, V	L243	BD Biosciences	FITC	5
CD138	II	MI15	BD Horizon	V450	2.5
IgM	II	G20-127	BD Pharmingen	APC	10
IgD	II	IA6-2	BD Pharmingen	FITC	5
CD21	II	B-ly4	BD Pharmingen	PE	5
CD27	II	M-T271	BD Pharmingen	PerCP-Cy5.5	2.5
CD45RA	III, IV, VI	HI100	BD Pharmingen	FITC, PerCP-Cy5.5	5
CD45RO	III, IV, V	UCHL1	BD Pharmingen	PerCP-Cy5.5	2.5
CCR3	III	5E8	BD Pharmingen	PE	2.5
CCR5	III, IV	2D7/CCR5	BD Pharmingen	PE-Cy7, PE	2.5, 5
CCR7	III, IV	3D12	BD Pharmingen	Alexa 647	2.5
CCR6	IV	11A9	BD Pharmingen	PE-Cy7	2.5
CD25	V	2A3	BD Biosciences	PE	5
CD127	V	HIL-7R-M21	BD Pharmingen	Alexa 647	5
TCR α/β	VI	WT31	BD Biosciences	FITC	5
CD31	VI	WM59	BD Pharmingen	PE	5
CD62L	VJ	DREG-56	BD Pharmingen	PE-Cy7	5
TCR γδ	VI	B1	BD Pharmingen	APC	5
CD94	VII	HP-3D9	BD Pharmingen	FITC	5
CD314 (NKG2D)	VII	1D11	BD Pharmingen	PE	5
CD161	VII	HP-3G10	BD Biosciences	BB700	2.5

Antibody	Panels	Clone	Vendor	Fluorophores	Antibody (uL)/100uL blood
CD122	VII	Mik-β3	BD Pharmingen	APC	5
CD57	VIII	HNK-1	BD Biosciences	FITC	5
NKp30 (CD337)	VIII	p30-15	BD Pharmingen	PE	5
NKp44 (CD336)	VIII	p44-8	BD Pharmingen	Alexa 647	10
NKp46 (CD335)	VIII	9E2/NKp46	BD Horizon	V450	2.5
TNF-α	Cytokine	MAb11	BD Pharmingen	PE	5*
IFN-γ	Cytokine	4S.B3	BD Pharmingen	PerCP-Cy5.5	5*
IL-2	Cytokine	MQ1-17H12	BD Horizon	BV510	5*
* The quantities of antibodies used for cytokine assays					

Cytokine secretion assay

The ability of cytokine secretion by B cells, T cells, and NK cells were detected by flow cytometry. Briefly, we diluted 100 μl of PBMCs with 400 μl of IMDM medium (Gibico-BRL, USA) in polystyrene tubes, and then stimulated the cells with or without leukocyte activation cocktail (BD GolgiPlug™, Germany) for 4 h at 37°C with 5% CO2. After stimulation, fluorochrome-conjugated lineage antibodies (Table 1) were added and incubated for 15 min at room temperature followed by lysis of RBCs. The cells were then fixed and permeabilized with 250 μl of Cytofix/Cytoperm (BD, Germany) at room temperature for 20 mins. After staining with fluorochrome-conjugated cytokine antibodies (Table 1) for 20 min at room temperature, the cell pellets were washed and re-suspend in 200 μl PBS. The FACS Canto II flow cytometer (BD Biosciences) and the FACS DIVA software (BD Biosciences) were used for data acquisition and analysis. The gated lymphocyte populations were further assessed for intracellular cytokine-producing cells. The levels of intracellular cytokines after stimulation were quantitatively determined from the percentage of lymphocytes with higher fluorescence intensity than cells without treatment.

Statistical analysis

All statistical analyses were performed using SPSS 17.0 for Windows (SPSS Inc. Chicago, IL). The significance of association between clinicopathologic variables was determined using the Chi-square and Fisher exact tests. The comparisons between two groups were performed using a Student's t-test. A two-sided test of significance was used and $P < 0.05$ was considered statistically significant. The lymphocyte subpopulations with a P-value < 0.01 were introduced into multiple linear regression models (as dependent variables) and tested against age, absolute lymphocyte counts, and groups.

Results

Clinicopathologic features

The median age was 61.6 years (range: 44.8–82.5 years) in the case group, and 45.5 years (range: 25.7–69.9 years) in the control group. Follow up was conducted with the patients for a median of 48 months (range: 3–125 months). All patients were Taiwanese except for a single patient who was from Vietnam. Table 2 summarizes the pertinent clinical presentation. Over four-fifths (17/20, 85%) of patients had the NTM infection, with three patients (3/17, 17.6%) infected by more than one species. The most frequently isolated NTM was *Mycobacterium abscessus*. Repeated infection was common among patients. Three species of NTM were isolated in Case 8 during sequential episodes of infection. The patient had obstruction and perforation of the jejunum due to a diffuse large B-cell lymphoma (DLBCL) (15 months after diagnosis). Skin manifestations were found in 14 patients (70%), including reactive skin conditions and infectious diseases. Cutaneous infection due to *Listeria monocytogenes* was found by culture in Case 19. The skin featured acute onset of generalized edematous erythema with nonfollicular sterile pustules. Twelve of 20 (60%) patients had infectious disease remission after completion of antibiotic treatment. Six (30%) patients received rituximab infusion, with three of them being free of infectious disease for more than 4 years. Furthermore, patients with rituximab infusion had a higher infectious disease remission rate than those without receiving the treatment [100% (6/6) versus 43% (6/14), $P = 0.04$].

Table 2
Clinicopathologic features of the patients with anti-IFN- autoantibodies

γ

Case	Age/sex	Associated infection	Site of involvement	Pattern of dermatosis	Histology of LN/detection of mycobacterium	Treatment with rituximab/recovery (months after completion of treatment)	Follow-up duration (months)
1	52/F	Disseminated M. abscessus infection, disseminated M. chimaera intracelluare infection, Salmonella sp. infection	Blood, lung, vertebra, soft tissue and breast	NA	NA	-/-	97
2	45/F	Pulmonry *Fonsecaea* sp infection, *Salmonella choleraaesuis* bacteremia, disseminated *M. abscessus* infection	Blood, lymph node, skin, bone and soft tissue	Direct skin and soft tissue infection	NGI/-	-/-	55
3	71/M	Disseminated *M. chimaera-intracellulare* infection	Lung, lymph node, skin and soft tissue	Direct skin and soft tissue infection	LH/-	-/-	53
4	70/M	*Salmonella sp. infection, M. abscessus lymphadenitis, Burkholderia gladioli bacteremia and deep neck infection*	Blood, lung, lymph node and soft tissue	Exanthematous pustulosis	SN/+	+/+ (7)	46
5	45/M	Disseminated tuberculosis, disseminated *M. chimaera-intracellular* group infection, *Salmonella enterica* serogroup D bacteremia	Blood, lung, bone marrow, spine, soft tissue	NA	LH/-	-/-	36
6	60/F	Disseminated *M. abscessus* infection	Lymph node and brain	NA	LH/-, SN/+, NGI/+	-/-	48
7	65/F	*Salmonella sp. infection, disseminated M. avium complex infection*	Lung, bone, soft tissue, and bone marrow	NA	NA	+/+ (71)	125
8	75/M	*M. hassiacum infection, M. parascrofulaceum infection, M. farcinogenes-senegalense* infection	Lung, bone, soft tissue, bone marrow and lymph node	Exanthematous pustulosis	NA	+/+ (2)	39

Y							
9	52/F	*Salmonella enterica* serogroup D bacteremia, *M. intracellulare* infection	Blood, nasophargynx, lung, lympho node, skin soft tissue	Exanthematous pustulosis, direct skin and soft tissue infection	NGI/-	+/+ (11)	89
10	73/F	Disseminated *M. intracelluare* infection	Lung, skin, lymph node, spine, bone marrow	NA	ALH/-	+/+ (48)	97
11	62/F	*Salmonella enterica* serogroup D infection, *M. fortuitum* lymphadenitis infection	Lymph node, brain	NA	NGI/+	+/+ (11)	73
12	48/F	*M. abscessus* infection, *M. kansasii* infection	Lymph node, spine	Exanthematous pustulosis, erythema nodosum and erythema induratum	NGI/+	-/+ (12)	65
13	65/M	Disseminated *M. abscessus* infection	Lymph node, spine	NA	ALH/+, SN/+	-/-	44
14	58/F	*Salmonella enterica* serogroup B bacteremia	Blood	NA	ALH/-	-/-	33
15	60/F	*Salmonella sp. bacteremia, M. abscessus infection*	Blood and lymph node	NA	NGI/+	-/+ (6)	11
16	72/M	*M. intracelluare* infection	Lung	Sweet's syndrome	NA	-/+ (9)	48
17	56/M	Disseminated *M. abscessus* infection	Nasopharynx, lymph node	Erythema nodosum	NGI/+	-/-	15
18	66/F	Disseminated *M. abscessus* infection	Lymph node	Sweet's syndrome	ALH/+, NGI/-	+/+ (51)	90
19	82/F	*Listeria monocytogenes* infection, *Salmonella choleraesuis* bacteremia	Blood and skin	Exanthematous pustulosis	NA	-/+ (6)	13
20	48/F	*Salmonella sp. infection*	Blood	NA	NA	-/+ (1)	3

ALH, atypical lymphoid hyperplasia; M., mycobacterium; NA, not available; NGI, necrotizing granulomatous inflammation; SN, suppurative necrosis; sp., species

Figure 1 depicts histopathology features of skin and lymph nodes, and the case with malignant lymphoma. Skin biopsies were available in 10 (50%) patients, seven with reactive skin disorders, two (Case 2 and Case 3) with granulomatous dermatoses and one (Case 9) with reactive lesions followed by granulomatous inflammation. Reactive lesions were mostly neutrophilic dermatoses such as exanthematous pustulosis, Sweet syndrome, and panniculitis. A total of 18 lymph nodes in 14 patients were available. Of these, eight of 18 samples (44.4%) were observed with necrotizing granulomatous inflammation, while three samples (16.7%) were found

with suppurative necrosis and lymphoid hyperplasia, respectively, whereas four (22.2%) samples had atypical lymphoid hyperplasia featuring a histiocytic response without granuloma formation. It should be noted that NTM infection was demonstrated by either acid-fast staining or culture in two patients (Case 13 and Case 18) with atypical lymphoid hyperplasia. Case 18 had elevated IgG4 levels and was misdiagnosed as angioimmunoblastic T-cell lymphoma initially [15]. Nevertheless, granulomatous inflammation of the lymph node was present in the repeat biopsy. Microscopically, atypical lymphoid hyperplasia showed irregularly thickening of the fibrous capsule and effaced nodal architecture with mixed lymphocytes, histiocytes, eosinophils, plasma cells, and few neutrophils. Malignant lymphoma was present in one case. Case 8 had a diffuse large B-cell lymphoma in the jejunum featuring transmural involvement of the bowel wall by large-sized lymphoma cells.

Distribution of subpopulations of peripheral blood lymphocytes

The flow cytometry gating strategy and representative immunophenotyping of lymphocyte subsets is shown in Fig. 2. Table 3 summarized the comparison of lymphocyte subpopulations based on flow cytometry data. The mean age of the patient group was significantly older than the healthy subjects. Percentages of constitutive T- and NK-cell subsets were significantly different between the case and control groups. Interactions between age, absolute lymphocyte counts, and groups (presence/absence of the disease) were determined using the multiple linear regression model. In Tables 4 and 5, longitudinal analysis of T lymphocyte subset distribution demonstrated that the case group showed significant and negative β coefficients for CD4 + T cells and non-activated subpopulations (RTEs and naïve subtypes). The ratios of CD4 + RTE/ CD4 + naïve T cells (0.5 ± 0.1 vs. 0.7 ± 0.1, $P = 0.002$) and CD8 + RTE/ CD8 + naïve T cells (0.9 ± 0.1 vs. 1.0 ± 0.1, $P = 0.011$) were significant lower. On the other hand, those relevant to activated T-cell subpopulations were positive and significant. The same model with NK-cell subsets as dependent variables highlighted that the case group showed significant and negative β coefficients for NK cells with either cytotoxic function or cytokine production and expression of Nkp30 and Nkp46, while that relevant to CD57 + NK cells was positive and significant (Table 6). The age β coefficient for naïve T cells and NK cells with expression of activation markers were negative and significant.

Table 3
Lymphocytes subpopulations in the patients with anti-IFN- autoantibodies and healthy controls

γ			
	Cases (N = 20)	Controls (N = 65)	*P* value
Age (yr)	61.4 ± 10.8	45.1 ± 12.3	< 0.001
Absolute lymphocytes counts ($\times 10^2$ cells/μL)	21.3 ± 8.3	20.0 ± 6.1	0.451
T cells (% lymphocytes)	52.7 ± 12.9	66.1 ± 9.4	< 0.001
α/β T cells (% T cells)	93.8 ± 4.3	90.0 ± 6.6	0.019
γδ T cells (% T cells)	4.8 ± 4.3	9.1 ± 6.5	0.006
CD4 + T cells (% T cells)	20.3 ± 6.9	33.9 ± 7.4	< 0.001
CD45RA + CD62L + CD31+ (% CD4 + cells)	7.8 ± 7.0	27.6 ± 9.9	< 0.001
Naïve (% CD4 + cells)	11.3 ± 8.6	34.3 ± 13.2	< 0.001
CD38 + HLA-DR+ (% CD4 + cells)	22.2 ± 15.8	4.5 ± 2.5	< 0.001
TCM (% CD4 + cells)	14.2 ± 6.1	16.3 ± 5.9	0.158
TEM (% CD4 + cells)	66.9 ± 12.1	37.8 ± 12.4	< 0.001
TE (% CD4 + cells)	3.6 ± 5.5	6.2 ± 5.1	0.051
Th1-like (% CD4 + cells)	48.6 ± 13.5	18.4 ± 9.7	< 0.001
Th2-like (% CD4 + cells)	12.1 ± 15.9	2.6 ± 3.3	0.015
Th17-like (% CD4 + cells)	39.4 ± 13.6	16.8 ± 6.3	< 0.001
CD8 + T cells (% T cells)	25.6 ± 8.0	26.7 ± 7.0	0.564
CD45RA + CD62L + CD31+ (% CD8 + cells)	5.2 ± 4.7	21.6 ± 10.6	< 0.001
Naïve (% CD8 + cells)	6.4 ± 5.6	29.4 ± 15.4	< 0.001
CD38 + HLA-DR+ (% CD8 + cells)	30.8 ± 17.0	14.5 ± 8.0	< 0.001
TCM (% CD8 + cells)	3.9 ± 4.4	1.7 ± 1.0	0.040
TEM (% CD8 + cells)	59.8 ± 12.5	39.4 ± 13.7	< 0.001
TE (% CD8 + cells)	21.8 ± 11.6	23.1 ± 13.5	0.694
TEM CCR5+ (% CD8 + cells)	38.7 ± 14.5	27.7 ± 10.7	< 0.001
TE CCR5+ (% CD8 + cells)	9.0 ± 8.8	8.4 ± 6.5	0.741
Regulatory T (Treg) cells (% T cells)	6.4 ± 3.6	5.1 ± 1.4	0.126
Naïve (% Treg cells)	19.2 ± 11.5	39.9 ± 12.5	< 0.001
Memory (% Treg cells)	80.8 ± 11.5	60.1 ± 12.5	< 0.001
HLA-DR+ (% Treg cells)	38.2 ± 23.6	14.7 ± 4.6	< 0.001
B cells (% lymphocytes)	8.8 ± 5.9	8.8 ± 3.9	0.955
Transitional (% B cells)	2.5 ± 2.0	2.5 ± 1.3	0.959
Naïve (% B cells)	61.7 ± 24.2	68.9 ± 13.5	0.216

Y			
Non-switched memory (% B cells)	9.4 ± 4.4	9.6 ± 5.7	0.864
Switched memory (% B cells)	8.0 ± 6.7	11.7 ± 6.0	0.019
$CD21^{low}CD38^{low}$ (% B cells)	6.4 ± 4.9	4.7 ± 4.1	0.126
Plasmablast (% B cells)	2.5 ± 4.1	1.6 ± 0.8	0.315
Plasma cell (% B cells)	2.7 ± 5.4	0.8 ± 0.7	0.140
NK cells (% lymphocytes)	40.0 ± 14.9	23.5 ± 9.7	< 0.001
$CD56^{bright}$ (% NK cells)	2.2 ± 1.2	4.5 ± 2.4	< 0.001
CD56 + CD16+ (% NK cells)	75.6 ± 10.6	93.2 ± 3.9	< 0.001
NKp30 (% NK cells)	22.4 ± 11.5	56.0 ± 15.6	< 0.001
NKp44 (% NK cells)	0.6 ± 0.4	0.6 ± 0.4	0.910
NKp46 (% NK cells)	12.9 ± 6.2	46.4 ± 16.1	< 0.001
CD57+ (% NK cells)	79.6 ± 7.9	57.4 ± 12.2	< 0.001
Data presented in means ± standard deviation; [a](×10^2 cells/μL)			
*Significance of the differences between cases and controls TCM, central memory T cell; TE, effector T cell; TEM, effector memory T cell; Th, T helper			

Table 4
Multiple linear regression analysis with CD4 + lymphocyte subpopulations as dependent variables

Variables	*B* (SE)	Beta	95% CI	*P*
CD4 + T cells (adjusted R^2 = 0.269)				
Age	0.075 (0.067)	0.129	-0.058, 0.209	0.264
Absolute lymphocytes counts	− .001 (0.001)	-0.058	− .003, 0.002	0.558
Group (case = 1; control = 0)	-11.259 (2.194)	-0.591	-15.633, -6.885	< 0.001
CD4 + CD45RA + CD62L + CD31 + RTE (adjusted R^2 = 0.474)				
Age	-0.215 (0.082)	-0.254	-0.379, -0.050	0.011
Absolute lymphocytes counts	0.000 (0.002)	0.017	-0.003, 0.003	0.843
Group (case = 1; control = 0)	-14.963 (2.703)	-0.541	-20.351, -9.575	< 0.001
CD4 + naïve T cells (adjusted R^2 = 0.421)				
Age	-0.271 (0.108)	-0.257	-0.487, -0.056	0.014
Absolute lymphocytes counts	0.000 (0.002)	0.008	-0.004, 0.004	0.924
Group (case = 1; control = 0)	-17.249 (3.542)	-0.499	-24.309, -10.189	< 0.001
CD4 + CD38 + HLA-DR + T cells (adjusted R^2 = 0.475)				
Age	0.023 (0.076)	0.029	-0.129, 0.175	0.763
Absolute lymphocytes counts	-0.002 (0.001)	-0.146	-0.005, 0.000	0.088
Group (case = 1; control = 0)	17.622 (2.506)	0.686	12.627, 22.618	< 0.001
CD4 + TEM (adjusted R^2 = 0.499)				
Age	0.133 (0.115)	0.11	-0.095, 0.362	0.249
Absolute lymphocytes counts	-0.001 (0.002)	-0.048	-0.006, 0.003	0.562
Group (case = 1; control = 0)	26.086 (3.762)	0.661	18.587, 33.586	< 0.001
Th1-like T cells (adjusted R^2 = 0.484)				
Age	0.004 (0.100)	0.004	-0.195, 0.203	0.967
Absolute lymphocytes counts	-0.001 (0.002)	-0.049	-0.005, 0.003	0.556
Group (case = 1; control = 0)	24.068 (3.278)	0.711	17.533, 30.603	< 0.001
Th17-like T cells (adjusted R^2 = 0.556)				
Age	-0.012 (0.080)	-0.013	-0.171, 0.148	0.885
Absolute lymphocytes counts	-0.001 (0.001)	-0.071	-0.004, 0.002	0.362
Group (case = 1; control = 0)	22.345 (2.617)	0.767	17.129, 27.562	< 0.001
Naïve Treg cells (adjusted R^2 = 0.342)				
Age	-0.182 (0.110)	-0.18	-0.402, 0.038	0.103
Absolute lymphocytes counts	-0.002 (0.002)	-0.07	-0.006, 0.003	0.459
Group (case = 1; control = 0)	-16.108 (3.617)	-0.487	-23.319, -8.897	< 0.001
Memory Treg cells (adjusted R^2 = 0.342)				

Variables	*B* (SE)	Beta	95% CI	*P*
Age	0.182 (0.110)	0.18	-0.038, 0.402	0.103
Absolute lymphocytes counts	0.002 (0.002)	0.07	-0.003, 0.006	0.459
Group (case = 1; control = 0)	16.108 (3.617)	0.487	8.897, 23.319	< 0.001
HLA-DR+ Treg cells (adjusted R^2 = 0.392)				
Age	-0.050 (0.118)	-0.044	-0.284, 0.185	0.674
Absolute lymphocytes counts	-0.001 (0.002)	-0.046	-0.005, 0.003	0.616
Group (case = 1; control = 0)	24.570 (3.854)	0.669	16.888, 32.252	< 0.001

B, unstandardized regression coefficient; Beta standardized regression coefficient; CI, confidence interval; RTE, recent thymic emigrants; SE, standard error

Table 5
Multiple linear regression analysis with CD8 + lymphocyte subpopulations as dependent variables

Variables	*B* (*SE*)	Beta	95% CI	*P*
CD8 + CD45RA + CD62L + CD31 + RTE (adjusted R^2 = 0.448)				
Age	-0.302 (0.079)	-0.381	-0.460, -0.145	< 0.001
Absolute lymphocytes counts	-0.001 (0.001)	-0.083	-0.004, 0.002	0.342
Group (case = 1; control = 0)	-10.373 (2.595)	-0.400	-15.546, -5.200	< 0.001
CD8 + naïve T cells (adjusted R^2 = 0.513)				
Age	-0.588 (0.109)	-0.505	-0.805, -0.370	< 0.001
Absolute lymphocytes counts	-0.003 (0.002)	-0.111	-0.007, 0.001	0.177
Group (case = 1; control = 0)	-12.080 (3.574)	-0.318	-19.205, -4.954	0.001
CD8 + CD38 + HLA-DR + T cells (adjusted R^2 = 0.294)				
Age	0.193 (0.104)	0.209	-0.015, 0.400	0.068
Absolute lymphocytes counts	0.001 (0.002)	0.037	-0.003, 0.005	0.706
Group (case = 1; control = 0)	12.954 (3.411)	0.430	6.153, 19.755	< 0.001
CD8 + TEM (adjusted R^2 = 0.333)				
Age	0.311 (0.123)	0.277	0.066, 0.555	0.014
Absolute lymphocytes counts	-0.001 (0.002)	-0.038	-0.005, 0.004	0.693
Group (case = 1; control = 0)	15.029 (4.026)	0.411	7.003, 23.054	< 0.001
CD8 + TEM CCR5+ (adjusted R^2 = 0.125)				
Age	0.036 (0.109)	0.041	-0.182, 0.253	0.742
Absolute lymphocytes counts	-0.002 (0.002)	-0.132	-0.007, 0.002	0.228
Group (case = 1; control = 0)	10.376 (3.577)	0.365	3.245, 17.507	0.005

B, unstandardized regression coefficient; Beta standardized regression coefficient; CI, confidence interval; RTE, recent thymic emigrants; SE, standard error

Table 6
Multiple linear regression analysis with lymphocyte subpopulations of NK cells as dependent variables

Variables	*B* (SE)	Beta	95% CI	*P*
NK cells (adjusted R^2 = 0.263)				
Age	0.197 (0.099)	0.229	0.000, 0.393	0.05
Absolute lymphocytes counts	0.002 (0.002)	0.134	-0.001, 0.006	0.183
Group (case = 1; control = 0)	10.141 (3.247)	0.362	3.687, 16.594	0.003
CD56 + bright NK cells (adjusted R^2 = 0.246)				
Age	-0.030 (0 .019)	-0.182	-0.067, 0.008	0.123
Absolute lymphocytes counts	-0.001 (0.000)	-0.255	-0.002, 0.000	0.014
Group (case = 1; control = 0)	-1.737 (0.623)	-0.326	-2.978, -0.496	0.007
CD56 + CD16 + NK cells (adjusted R^2 = 0.604)				
Age	0.027 (0.059)	0.038	-0.090, 0.143	0.652
Absolute lymphocytes counts	-0.002 (0.001)	-0.113	-0.004, 0.000	0.126
Group (case = 1; control = 0)	-17.847 (1.923)	-0.787	-21.680, -14.014	< 0.001
Nkp30 + NK cells (adjusted R^2 = 0.551)				
Age	-0.444 (0.130)	-0.309	-0.703, -0.186	0.001
Absolute lymphocytes counts	-0.003 (0.002)	-0.094	-0.008, 0.002	0.230
Group (case = 1; control = 0)	-25.335 (4.246)	-0.538	-33.799, -16.871	< 0.001
Nkp46 + NK cells (adjusted R^2 = 0.567)				
Age	-0.378 (0.123)	-0.271	-0.624, -0.133	0.003
Absolute lymphocytes counts	-0.003 (0.002)	-0.111	-0.008, 0.001	0.152
Group (case = 1; control = 0)	-26.299 (4.043)	-0.576	-34.359, -18.240	< 0.001
CD57 + NK cells (adjusted R^2 = 0.464)				
Age	0.190 (0.103)	0.182	-0.015, 0.395	0.069
Absolute lymphocytes counts	0.003 (0.002)	0.117	-0.001, 0.006	0.176
Group (case = 1; control = 0)	19.459 (3.371)	0.569	12.74, 26.179	< 0.001

B, unstandardized regression coefficient; Beta standardized regression coefficient; CI, confidence interval; SE, standard error

In order to reflect the real immune status in patients with anti-IFN-γ autoantibodies, we compared immunological data of 12 cases leaving antimicrobial therapy with 18 age-matched healthy individuals. The median of age was 64.5 years (range: 47.9–82.5 years) in the case group and 60.6 years (range: 54.5–69.9 years) in the control group. Statistical significance of differences in the lymphocyte subsets between the groups remained similar (Supplementary Table 1). The mean percentages of T cells (50.0 ± 14.6 vs. 65.8 ± 8.6, P = 0.004), CD4 + T cells (20.3 ± 6.9 vs. 33.9 ± 7.4, P < 0.001), CD4 + RTE (7.6 ± 5.4 vs. 21.8 ± 8.2, P < 0.001), CD8 + RTE (5.2 ± 4.5 vs. 15.8 ± 6.6, P < 0.001), $CD5^{bright}$ NK cells (2.1 ± 1.1 vs. 4.5 ± 2.9, P = 0.004), CD56 + CD16 + NK cells (77.0 ± 12.7 vs. 93.8 ± 3.4, P < 0.001), Nkp30 + NK cells (19.4 ± 11.1 vs. 49.0 ± 11.2, P < 0.001), and Nkp46 + NK cells (12.3 ± 6.1 vs. 40.3 ± 11.4, P < 0.001) were lower in the case group. Nevertheless, the levels of CD4 + CD38 + HLA-DR + T cells (18.3 ± 14.8 vs. 4.8 ± 1.4, P = 0.009), CD4 + TEM (64.8 ± 9.0 vs. 41.6 ± 11.4, P < 0.001), Th1-like subtype (40.5 ± 10.7 vs. 20.4 ± 7.3, P < 0.001), Th17-like subtype (33.6 ± 9.4 vs. 19.5 ± 5.5, P < 0.001), and CD57 + NK cells (80.9 ± 7.2 vs. 59.0 ± 11.2, P < 0.001) were higher in the case group. CD8 + CD38 + HLA-DR+ (29.3

± 16.0 vs. 16.4 ± 10.2, $P = 0.025$) and CD8 + TEM (56.6 ± 11.6 vs. 45.2 ± 14.5, $P < 0.024$) T cells had a marginally significant increase in the patient group.

Production of cytokines in lymphocyte subpopulations

We then tested production of intracellular cytokines of PBMCs that were free of autologous plasma to determine cell-intrinsic functions (Fig. 3). Among lymphocytes subpopulations, expressions of TNF-α and IFN-γ were relatively evident in CD4+ (TNF-α, median: 2.2%, range: 0–15.8%; IFN-γ, median: 8.2%, range: 0.7–28.6%) and CD8+ (TNF-α, median: 2.6%, range: 0–14.4%; IFN-γ, median: 11.6%, range: 0.6–32.3%) T cells in the patient group. Secretion of IL-2 was restricted in the CD4 + subset (median: 2.8%, range: 0–32.9%). When compared with the control group, the percentages of TNF-α-producing CD4 + T cells ($P = 0.009$), CD8 + T cells ($P < 0.001$), and NK cells ($P = 0.002$) were significantly lower in the case group. IFN-γ-producing cells were decreased in CD8 + T-cell ($P = 0.002$) and NK-cell ($P = 0.001$) subpopulations. The percentages of IL-2-producing CD4+ ($P < 0.001$), and CD8+ ($P = 0.005$) T cells were also significantly lower. Similar differences were identified when comparing patients with discontinuing antibiotic therapy and age-matched healthy controls.

Discussion

Our data clarify the clinicopathologic and immunological features in patients with anti–IFN-γ Abs. We confirmed that the patients experienced recurrent infection, particularly NTM and skin dermatoses. An unspecific clinical presentation of primary DLBCL in the jejunum and NTM lymphadenitis without granuloma formation was observed. A limitation of the present study included the heterogeneous patient group, who were in various infectious statuses, such as active, inactive, or chronic. We were also unable to exclude the action of corticosteroid which may be prescribed for these patients on lymphocyte subset levels. However, we compared immunological data of 12 cases leaving antimicrobial therapy with 18 age-matched healthy individuals to diminish the effect of diverse clinical conditions on the data. The T cells were activated with polarization to Th1, Th17, and Treg. Lower ratios of RTE cells to naïve T cells might be indicate of lower thymic output in these patients. Although the number of NK cells was increased as in previous reports [1, 10], the percentages of subsets expressing activating markers were decreased. Upon stimulation, cytokine expression in T and NK cells was lower when compared with the control group.

IFN-γ plays an important role in granuloma formation for mycobacterial infection. Recurrent NTM infection is one of the most important clinicopathological features in patients with anti–IFN-γ Abs. For early diagnosis, histologic examination and acid-fast staining may be helpful. Microscopically, four histologic patterns have been detected [16]. That includes necrotizing and non-necrotizing granulomas, suppurative granulomas, and a histologic response lacking granulomas. In our study, 16.7% of patients with anti–IFN-γ Abs had suppurative necrosis with limited granuloma formation in lymph nodes. In addition, 22.2% of patients showed a mixture of large pale histiocytes, lymphocytes, plasma cells, and few granulocytes. No granulomas were detected. The effective immune response generated by IFN-γ in response to mycobacterial infection to form granulomas seems defected due to the presence of neutralizing anti-IFN-γ Abs, and it is necessary to maintain a high index suspicion of mycobacterial infection in such patients.

Administration of anti-CD20 monoclonal antibody (rituximab) has been reported to effectively reduce autoantibody titers, improve IFN-γ signaling, and achieve clinical remission [17–19]. Browne et al. was the first to demonstrate 4 patients treated with rituximab against refractory disseminated NTM [20]. After treatment with rituximab, the clearance of infection, resolution of inflammation, and reduction of autoantibody titers were improved. Furthermore, IFN-γ–induced STAT-1 phosphorylation was preserved. In the present study, the patients with rituximab therapy had more opportunities to discontinue antibiotic therapy. This treatment strategy seemed reasonable because of the unique mechanism by which rituximab attacks CD20 positive cells involved in antibody production. However, long-term follow-up data is limited. Despite rituximab administration, refractory and relapsed cases were also reported [7, 21]. Further research is necessary to evaluate the outcome of anti-CD20 therapy.

Current understanding of immune dysfunction in patients with anti–IFN-γ Abs is limited. In a study conducted by Browne et al., lymphocyte phenotyping showed a significantly decreased T cell percentage and naïve T lymphocytes, which was consistent with our results [1]. In addition, we found that the percentages of T cells with activation and polarization to Th1-like and Th17-like subsets were increased, based on dynamic analysis of T cell subpopulations. It raises the question whether decreased non-activated T cell subpopulations are age- or disease-related thymic impairments or just a dynamic fluctuation of T-cell subsets due to infection. To objectively evaluate the thymic function, the percentage of RTEs representative of the youngest T cells in the PBMCs were detected

and analyzed with or without age adjustment. The ratio of RTE to naïve T subsets was compared between the disease and control groups to clarify thymic output during dynamic changes that occur during the immune response. Our data suggested that patients with anti-IFN-γ Abs would have lower levels of RTEs in the peripheral T-cell pool. This may impact the replenishment and diversity of T cells, and result in a delayed regeneration of T cells with a broad TCR repertoire [22].

Furthermore, an expansion of CD38 + HLA-DR + T cells was detected in the case group. High expressions of CD38 + HLA-DR + CD4 + and CD38 + HLA-DR + CD8 + T-cell subsets, indicative of T-cell activation, are well-known in viral and bacterial infections [23–25]. However, repetitive or prolonged antigen stimulation may induce expression of exhaustion markers and decrease IFN-γ production [26]. Wang et al. demonstrated patients with fatal H7N9 outcomes displayed higher and prolonged expression of CD38 + HLA-DR + on CD8 + T cells than those who survived [24]. The majority of these activated T cells concurrently expressed high levels of PD-1 with minimal IFN-γ production. In addition, a delay of clonally expanded TCRαβ clonotypes within CD38 + HLA-DR + CD8 + T cells were featured in fatal cases. Similarly, our data revealed higher percentages of CD38 + HLA-DR + CD4 + and CD38 + HLA-DR + CD8 + T cells in the patients with anti-IFN-γ Abs. These patients suffered from adult-onset immunodeficiency due to defects in IFN-γ immune surveillance that may lead to recurrent infection. While the status of PD-1 expression was not examined, the decreased expression of intracellular cytokines in the disease group supported exhausted function in these T cells.

In agreement with previous studies, the number of NK cells was increased in patients with anti-IFN-γ Abs [1, 10]. Chronic and repeating opportunistic infections may be the predominant cause for the increase of NK cells. We further evaluated subpopulations and functional markers of NK cells. Two major NK subpopulations, $CD56^{bright}$ and CD56 + CD16 + subsets were decreased. Expression of CD57 was increased when comparing the patients with the healthy subjects. Moreover, the NK cells diminished the expression of NKp30 and NKp46 and the production of TNF-α and IFN-γ. Indeed, CD56 + CD16 + NK cells with a high cytolytic potential differentiate from $CD56^{bright}$ NK cells, which proliferate and produce IFN-γ in response to stimulation [27, 28]. CD57 cells define a subset of highly mature cells in the NK population [29]. The expression of activation receptors, including NKG2D, DAP10, CD16, natural cytotoxicity receptors (NKp30, NKp44, and NKp46), CD226, and 2B4 are downregulated during NK-cell maturation [30]. NK cells exhibiting impaired effector functions have also been reported in hosts with tumors or chronic infections [31]. NK cells with exhausted effector functions show decreased cytokine production and cytolytic activity. Altogether, theses data indicate the exhausted immune status of NK cells in patients with anti-IFN-γ Abs. Further study is necessary to clarify the functional exhaustion in the expanded CD57 + subpopulation.

The study of the ability of lymphocyte subpopulations to produce cytokines in patients with anti-IFN-γ Abs is limited. While engulfing mycobacteria, mononuclear phagocytes secret IL-12 to activate T- and NK-cells and introduce IFN-γ production. The IFN-γ biding signals enable macrophage activation with upregulation of expressions of TNF-α and IL-12 through phosphorylated STAT1- and NFκB essential modulator-mediated pathways [2]. TNF-α and IFN-γ are essential for granuloma formation, which is hallmark of a mycobacterial infection. Anti-IFN-γ Abs may block production of downstream mediators of IFN-γ activity. Krisnawati et al. reported a significant decrease in levels of serum TNF-α and IFN-γ in all tested sera of patients with anti-IFN-γ Abs [9]. Production of IL-2 and TNF-α in CD4 + cells and TNF-α in CD8 + cells was significantly lower in a study conducted by Wipasa et al. [11]. The present study found similar results, with a decrease in cytokine production in lymphocyte subpopulations. That may explain the lack of formation of granulomas in some patients, although the cytokine production varied a great deal. On the other hand, the reduction of cytokine responses may account for immune exhaustion and lead to a higher risk of disseminated NTM or other opportunistic infections, like patient 19 who was infected by *L. monocytogenes*.

Conclusions

In conclusion, we reported on clinicopathologic features and the immune status of 20 patients with anti–IFN-γ Abs. This study demonstrated that NTM-associated lymphadenitis could develop without granuloma formation, and that DLBCL could occur in the unusual site. Additionally, T cells were activated with decreased thymic output, and NK cells were highly matured with diminished expression of activation markers. The lymphocyte subpopulations had the reduction of cytokine responses, and therefore, were likely to be suggestive of the immune system being exhausted in these patients. We believe our study has shed light on the pathogenesis of the reported disease which presents recurrent infection.

Declarations

Funding This study was supported by the Chang Gung Memorial Hospital (grant number CMRPG8K0341).

Conflicts of Interest The authors declare no competing interests.

Availability of data and material Upon request.

Code availability Upon request

Acknowledgements We acknowledge Mr. Yu-Shiang Hu (senior product specialist, BD Biosciences, Taiwan) for help with the experimental setting.

Authors' Contributions WTH conceptualized and designed the study. WCH and HLY acquired the data. YCC, CHL, and WTH interpreted the data. YCC and WTH conducted the literature review and wrote the manuscript draft. SWW performed the statistical analysis. All authors critically reviewed and approved the final manuscript.

Ethics approval This study was approved by the Ethics Committee of Chang Gung Memorial Hospital, Kaohsiung, Taiwan, in accordance with the Declaration of Helsinki (IRB201901509B0C501).

Consent to participate All participants gave informed written consent.

Consent for publication Obtained

References

1. Browne SK, Burbelo PD, Chetchotisakd P, Suputtamongkol Y, Kiertiburanakul S, Shaw PA, et al. Adult-onset immunodeficiency in Thailand and Taiwan. N Engl J Med. 2012;367(8):725–34
2. Wu UI, Holland SM. Host susceptibility to non-tuberculous mycobacterial infections. Lancet Infect Dis. 2015;15(8):968–80
3. Ku CL, Chi CY, von Bernuth H, Doffinger R. Autoantibodies against cytokines: phenocopies of primary immunodeficiencies? Hum Genet. 2020;139(6–7):783–94
4. Hong GH, Ortega-Villa AM, Hunsberger S, Chetchotisakd P, Anunnatsiri S, Mootsikapun P, et al. Natural history and evolution of anti-interferon-gamma autoantibody-associated immunodeficiency syndrome in Thailand and the United States. Clin Infect Dis. 2020;71(1):53–62
5. Jutivorakool K, Sittiwattanawong P, Kantikosum K, Hurst CP, Kumtornrut C, Asawanonda P, et al. Skin manifestations in patients with adult-onset immunodeficiency due to anti-interferon-gamma autoantibody: A relationship with systemic infections. Acta Derm Venereol. 2018;98(8):742–7
6. Wu UI, Wang JT, Sheng WH, Sun HY, Cheng A, Hsu LY, et al. Incorrect diagnoses in patients with neutralizing anti-interferon-gamma-autoantibodies. Clin Microbiol Infect. 2020;26(12):1684:e1–e6
7. Koizumi Y, Mikamo H. Anti-Interferon-gamma autoantibody and disseminated nontuberculous mycobacteria infection. What should be done to improve its clinical outcome? Clin Infect Dis. 2020
8. Page AV, Liles WC. Immunomodulators. In: Bennett JE, Dolin R, Blaser MJ. Mandell, douglas, and bennett's principles and practice of infectious diseases: 2-volume set: Elsevier Health Sciences; 2014. pp.627-54
9. Krisnawati DI, Liu YC, Lee YJ, Wang YT, Chen CL, Tseng PC, et al. Functional neutralization of anti-IFN-gamma autoantibody in patients with nontuberculous mycobacteria infection Sci. rep.:2019:9(1):5682
10. Chruewkamlow N, Mahasongkram K, Pata S, Chaiwarith R, Salee P, Supparatpinyo K, et al. Immune alterations in patients with anti-interferon-gamma autoantibodies. PLOS ONE. 2016;11(1):e0145983
11. Wipasa J, Wongkulab P, Chawansuntati K, Chaiwarit R, Supparatpinyo K. Cellular immune responses in HIV-negative immunodeficiency with anti-interferon-gamma antibodies and opportunistic intracellular microorganisms. PLOS ONE. 2014;9(10):e110276
12. Chi CY, Chu CC, Liu JP, Lin CH, Ho MW, Lo WJ, et al. Anti-IFN-gamma autoantibodies in adults with disseminated nontuberculous mycobacterial infections are associated with HLA-DRB1*16:02 and HLA-DQB1*05:02 and the reactivation of latent varicella-zoster virus infection. Blood. 2013;121(8):1357–66

13. Chi CY, Lin CH, Ho MW, Ding JY, Huang WC, Shih HP, et al. Clinical manifestations, course, and outcome of patients with neutralizing anti-interferon-gamma autoantibodies and disseminated nontuberculous mycobacterial infections. Med (Baltim). 2016;95(25):e3927
14. Boldt A, Borte S, Fricke S, Kentouche K, Emmrich F, Borte M, et al. Eight-color immunophenotyping of T-, B-, and NK-cell subpopulations for characterization of chronic immunodeficiencies. Cytometry B Clin Cytom. 2014;86(3):191–206
15. Liu TT, Weng SW, Wang MC, Huang WT. Nontuberculous mycobacterial infection with concurrent IgG4-related lymphadenopathy. APMIS. 2016;124(3):216–20
16. Shah KK, Pritt BS, Alexander MP. Histopathologic review of granulomatous inflammation. J Clin Tuberc Other Mycobact Dis. 2017;7:1–12
17. Czaja CA, Merkel PA, Chan ED, Lenz LL, Wolf ML, Alam R, et al. Rituximab as successful adjunct treatment in a patient with disseminated nontuberculous mycobacterial infection due to acquired anti-interferon-gamma autoantibody. Clin Infect Dis. 2014;58(6):e115–8
18. Hase I, Morimoto K, Sakagami T, Ishii Y, van Ingen J. Patient ethnicity and causative species determine the manifestations of anti-interferon-gamma autoantibody-associated nontuberculous mycobacterial disease: a review. Diagn Microbiol Infect Dis. 2017;88(4):308–15
19. Koizumi Y, Sakagami T, Nishiyama N, Hirai J, Hayashi Y, Asai N, et al. Rituximab restores IFN-gamma-STAT1 function and ameliorates disseminated *Mycobacterium avium* infection in a patient with anti-interferon-gamma autoantibody. J Clin Immunol. 2017;37(7):644–9
20. Browne SK, Zaman R, Sampaio EP, Jutivorakool K, Rosen LB, Ding L, et al. Anti-CD20 (rituximab) therapy for anti-IFN-gamma autoantibody-associated nontuberculous mycobacterial infection. Blood. 2012;119(17):3933–9
21. Ochoa S, Ding L, Kreuzburg S, Treat J, Holland SM, Zerbe CS. Daratumumab (anti-CD38) for treatment of disseminated nontuberculous mycobacteria in a patient with anti-IFN-gamma autoantibodies. Clin Infect Dis. 2020
22. Moore JW, Beattie L, Osman M, Owens BM, Brown N, Dalton JE, et al. CD4+ recent thymic emigrants are recruited into granulomas during *Leishmania donovani* infection but have limited capacity for cytokine production. PLOS ONE. 2016;11(9):e0163604
23. Lim A, Allison C, Tan DB, Oliver B, Price P, Waterer G. Immunological markers of lung disease due to non-tuberculous mycobacteria. Dis Markers. 2010;29(2):103–9
24. Wang Z, Zhu L, Nguyen THO, Wan Y, Sant S, Quiñones-Parra SM, et al. Clonally diverse CD38+HLA-DR+CD8+ T cells persist during fatal H7N9 disease. Nat Commun. 2018;9(1):824
25. Gonzalez SM, Taborda NA, Rugeles MT. Role of different subpopulations of CD8+ T cells during HIV exposure and infection. Front Immunol. 2017;8:936
26. Fink PJ. The biology of recent thymic emigrants. Annu Rev Immunol. 2013;31:31–50
27. Michel T, Poli A, Cuapio A, Briquemont B, Iserentant G, Ollert M, et al. Human CD56bright NK cells: an update. J Immunol. 2016;196(7):2923–31
28. Batoni G, Esin S, Favilli F, Pardini M, Bottai D, Maisetta G, et al. Human $CD56^{bright}$ and $CD56^{dim}$ natural killer cell subsets respond differentially to direct stimulation with *Mycobacterium bovis* bacillus Calmette-Guerin. Scand J Immunol. 2005;62(6):498–506
29. Lopez-Vergès S, Milush JM, Pandey S, York VA, Arakawa-Hoyt J, Pircher H, et al. CD57 defines a functionally distinct population of mature NK cells in the human $CD56^{dim}$CD16+ NK-cell subset. Blood. 2010;116(19):3865–74
30. Long EO, Kim HS, Liu D, Peterson ME, Rajagopalan S. Controlling natural killer cell responses: integration of signals for activation and inhibition. Annu Rev Immunol. 2013;31:227–58
31. Bi J, Tian Z. NK cell exhaustion. Front Immunol. 2017;8:760

Figures

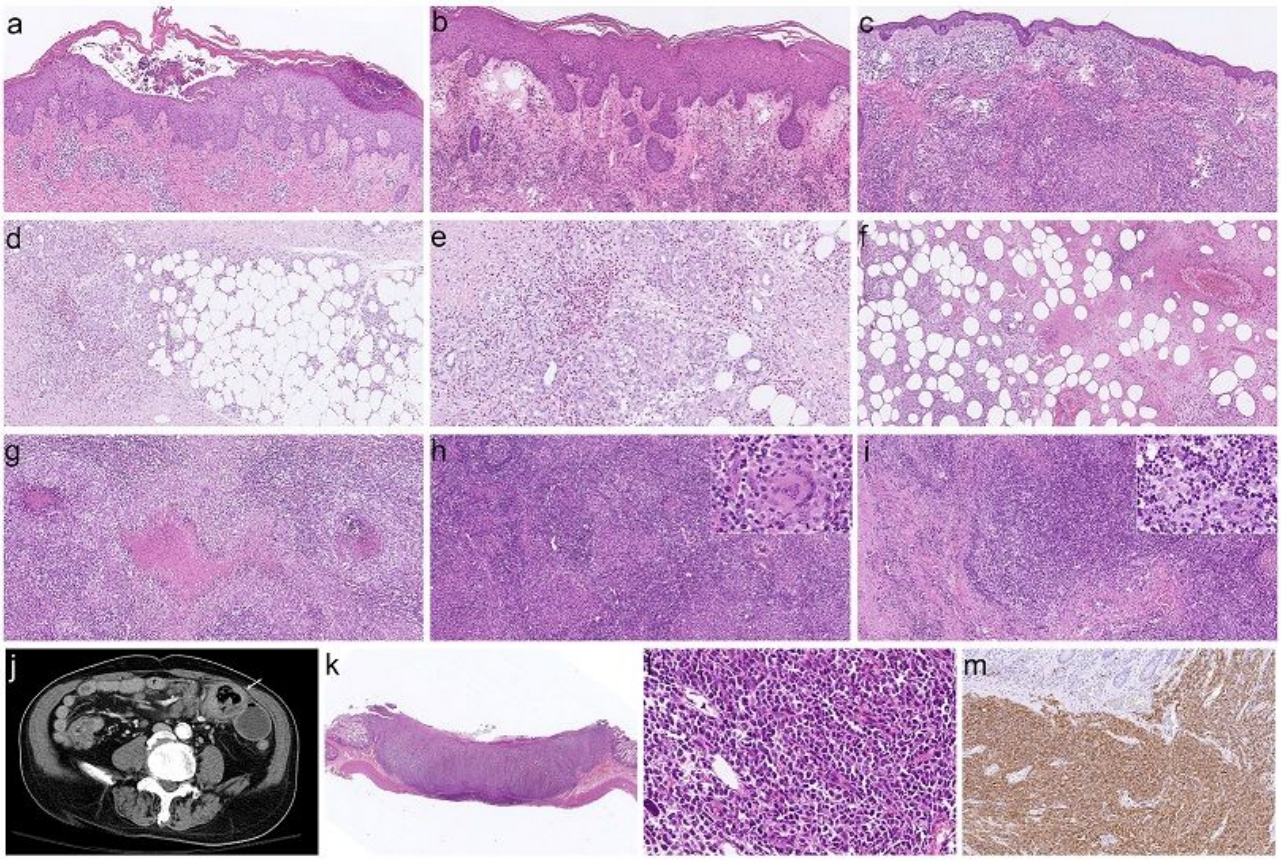

Figure 1

Histopathologic features in patients with anti-IFN-γ autoantibodies. Representative hematoxylin and eosin (H&E) of the skin biopsy shows subcorneal and intraepidermal collections of neutrophils (a), a dense neutrophilic infiltration in the dermis (b), granulomatous inflammation (c), erythema nodosum featuring both septal and lobular infiltrates of lymphocytes, neutrophils, histiocytes, eosinophils and granulomas with giant cells (d,e), and erythema induratum characterized by predominantly lobular panniculitis with histiocytes forming granulomas, necrosis and vasculitis (f). Histologic features of the lymph node reveal necrotizing granulomatous inflammation (g), vague granulomas (h), and atypical lymphoid proliferation (inset figure) with thickened capsule (i). The computed tomography scan with intravascular contrast enhancement in case 8 shows spiculated wall thickening of the jejunum (arrow) with small bowel obstruction (j). The H&E demonstrates transmural involvement of the bowel wall (k) by infiltrates of large lymphoid cells (l), which showing positive CD20 staining (m).

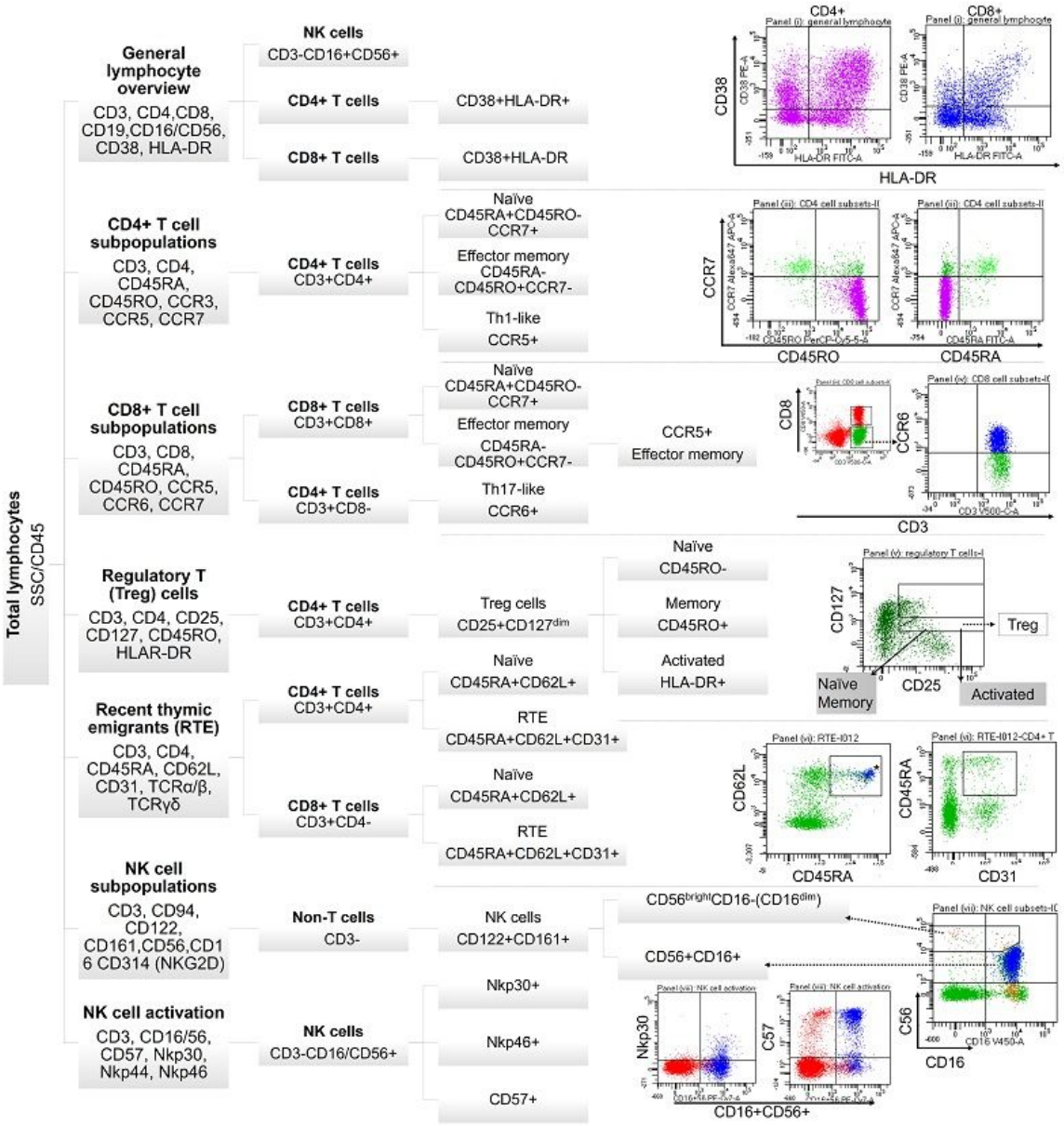

Figure 2

Representative flowchart diagram of immunophenotyping results by flow cytometry in patients with anti-IFN-γ autoantibodies. The flowchart starting with the delineation of lymphocytes using side scatter versus CD45 dot plots is followed by the major steps drawn vertically to discriminate between specific cell populations. The most basic steps in this process list all markers used to assess lymphocyte subpopulations. Under each step, the sub-steps are listed in the following order: CD4+ T cells, CD8+ T cells, and NK cells with respective subset populations.* Dot plots in the inset indicating naïve T-cells and those with the selective expression of CD31 (blue) by the use of the AND operator to combine two individual gates.

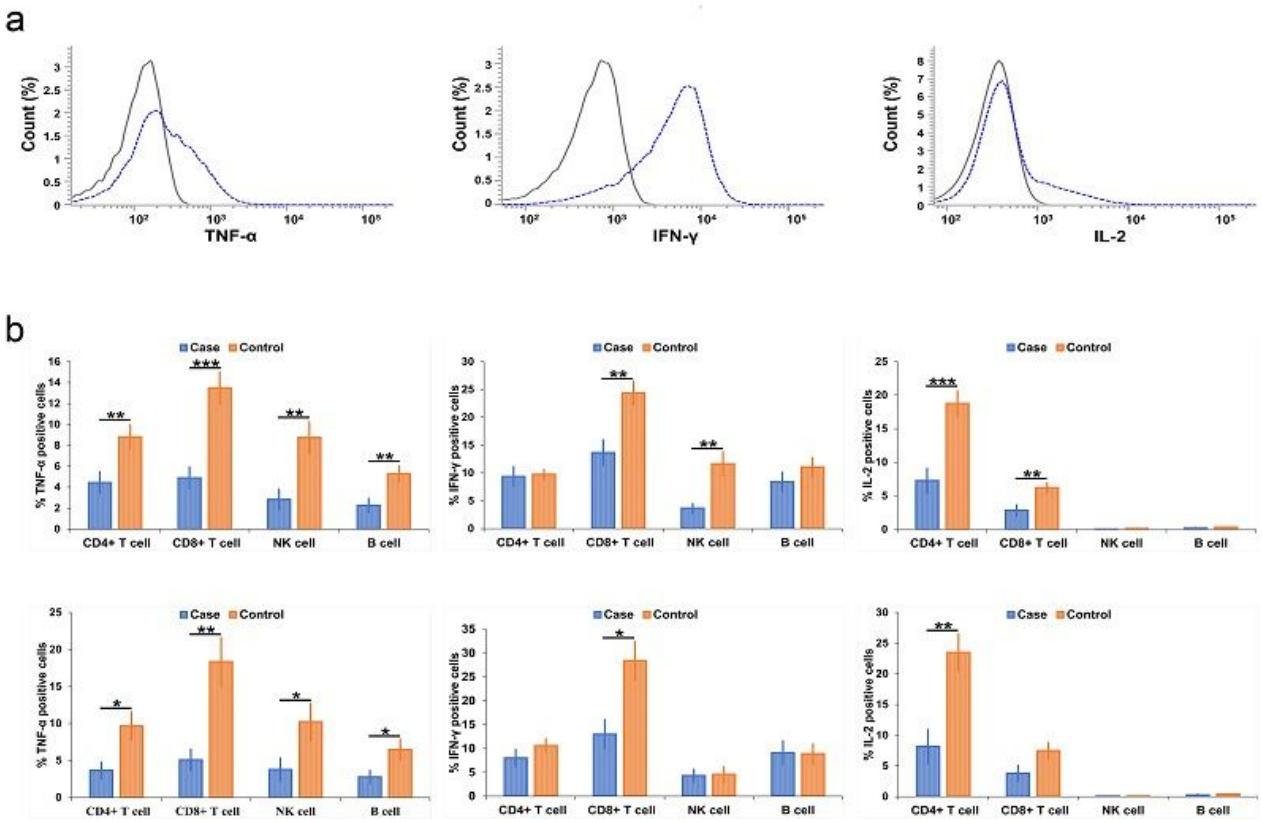

Figure 3

Intracellular cytokine production of patients with anti-IFN-γ auto-antibody and healthy subjects. Peripheral blood mononuclear cells (PBMCs) were stimulated with a leukocyte activation cocktail. The PBMCs were then stained using APC-H7 conjugated anti-CD45 antibody, FITC conjugated anti-CD3 antibody, BV421 conjugated anti-CD4 antibody, APC conjugated anti-CD8 antibody, PE-Cy7 conjugated anti-CD16/anti-CD56 antibodies, PE conjugated anti-TNF-α antibody, PerCP-Cy5.5 conjugated anti-IFN-γ antibody, and BV510 conjugated anti- IL-2 antibody. The upper panel is representative of figures of the cytokine production in CD8+ T cells (a). The increase in the cytokine production in response to the stimulant (blue dash curve) as compared to the baseline with no stimulant (gray solid curve) was calculated. The results are represented as percentage of lymphocytes with the fluorescent intensity higher than the baseline (b). The upper column is comparison data from 20 cases and 65 healthy subjects, and the lower from 12 cases leaving therapy and 18 age-matched healthy subjects. Data represent means ± standard error of mean. “*” represents $P < 0.05$; “**” represents $P < 0.01$; “***” represents $P < 0.001$.

Supplementary Files

This is a list of supplementary files associated with this preprint. Click to download.

- SupplementaryTable1.docx